Received: 5 November 2017 | Revised: 22 January 2018 | Accepted: 2 February 2018

DOI: 10.1002/qua.25608

FULL PAPER

WILEY International Journal of QUANTUM CHEMISTRY

NMR spin–spin coupling constants in hydrogen-bonded glycine clusters

Puspitapallab Chaudhuri[1,2] | **Sylvio Canuto**[2] | **Patricio F. Provasi**[3]

[1]Department of Physics, Federal University of Amazonas, 69077-000 Manaus, AM, Brazil

[2]Department of General Physics, Institute of Physics, University of São Paulo, 05508-090, São Paulo, SP, Brazil

[3]Department of Physics - IMIT, Northeastern University - CONICET, W 3404 AAS Corrientes, Argentina

Correspondence
Puspitapallab Chaudhuri, Department of Physics, Federal University of Amazonas, 69077-000 Manaus, AM, Brazil.
Email: puspito@ufam.edu.br

Funding information
Brazilian funding agency CNPq; CONICET and UNNE, Grant/Award Number: PI:15/F002 Res. 1017/15

Abstract

The influence of the hydrogen bond formation on the NMR spin–spin coupling constants (SSCC), including the Fermi contact (FC), the diamagnetic spin-orbit, the paramagnetic spin-orbit, and the spin dipole term, has been investigated systematically for the homogeneous glycine cluster, in gas phase, containing up to three monomers. The one-bond and two-bond SSCCs for several intramolecular (through covalent bond) and intermolecular (across the hydrogen-bond) atomic pairs are calculated employing the density functional theory with B3LYP and KT3 functionals and different types of extended basis sets. The ab initio SOPPA(CCSD) is used as benchmark for the SSCCs of the glycine monomer. The hydrogen bonding is found to cause significant variations in the one-bond SSCCs, mostly due to contribution from electronic interactions. However, the nature of variation depends on the type of oxygen atom (proton-acceptor or proton-donor) present in the interaction. Two-bond intermolecular coupling constants vary more than the corresponding one-bond constants when the size of the cluster increases. Among the four Ramsey terms that constitute the total SSCC, the FC term is the most dominant contributor followed by the paramagnetic spin-orbit term in all one-bond interaction.

KEYWORDS

DFT, glycine, hydrogen bond, SOPPA (CCSD), spin–spin coupling constant

1 | INTRODUCTION

Glycine (with chemical formula NH_2CH_2COOH) is the simplest naturally occurring amino acid. Unlike other amino acids, glycine (abbreviated as GLY henceforth in this article) contains just a single hydrogen atom as side-chain, which makes it highly flexible from the structural point of view. This structural flexibility, conversely, helps GLY to play vital functional role in the maintenance of conformational stability of proteins. Because of its many important biochemical and physiological activities that include interorgan metabolic regulations, anti-oxidative reactions, and neurological function, GLY is frequently studied in the areas of biotechnology, biomedical, and agricultural sciences. In quantum chemistry related areas, GLY is regularly used as a suitable model molecule to investigate different biomolecular structures, properties, and interactions, both experimentally and theoretically.[1–12] Applications of different quantum chemical methods to study different properties of this model molecule is also helpful, as a by-product, in assessing the quality of different theoretical approaches. The importance of GLY, in fact, goes far beyond the terrestrial limit as intense search is on to find it definitively in the extraterrestrial atmosphere.[13–18] Identification of interstellar glycine in the direction of the hot molecular cores Sgr B2(N-LMH), Orion KL, and W51 e1/e2 has already been reported,[17] although it became a debatable issue.[18] However, detection of glycine in comets and their coma is confirmed by now.[19,20]

In recent years, nuclear magnetic resonance (NMR) has turned into a powerful tool for investigating biomolecular structures in different environments. In the area of high resolution NMR spectroscopy, investigation of spin–spin coupling constants (SSCC) is very important since these experimentally measurable parameters may provide very useful information about the structural and conformational characteristics of molecules and their complexes. Conversely, the formation of hydrogen bond (H-bond) is essential in the stabilization of many molecular clusters and complex multiatomic molecular structures in chemical and biological environments. Since H-bonded interactions affect the electron density of the participating

atoms, SSCCs can be useful in the detection and analysis of the nature of hydrogen bonds. A significant progress regarding the calculation of the SSCCs for H-bonded molecular systems has been made in last few years.[21–34]

Several highly sophisticated correlation-consistent wavefunctions-based methods like the multiconfigurational self-consistent field (MCSCF) theory,[35–38] second-order polarization propagator approach (SOPPA),[39–42] Equation of motion coupled cluster with single and double excitation (EOM-CCSD),[43–45] iterative approximate coupled cluster singles, doubles, and triples (CC3) model[46–48] have been developed, in last few decades, to study the electronic structure of molecular systems. These first-principle correlation-consistent methods, although predict the SSCCs quite accurately, they are generally costly from the computational point of view. Thus, applications of these methods are limited in most cases to small molecular systems. Density functional theory (DFT)-based methods utilizing hybrid functionals, conversely, have emerged as suitable alternative to the traditional first-principle theories as it allows to treat relatively large molecules with relative ease providing a good compromise between computational cost and numerical accuracy. They are being routinely tested and utilized to calculate SSCCs and other NMR parameters of different types of molecular systems.[23,31,49–57]

Despite the structural simplicity, GLY is capable of forming complex H-bonded networks as it possesses multiple sites available for H-bonding. With the help of the polar C═O, C—O, O—H, and N—H bonds, it can form the conventional O—H···O or N—H···O type H-bonds with other molecules like water. Conversely, it can also form nonconventional C—H···O type H-bond through the C^{α}—H bond, which, albeit weaker than conventional H-bond, plays important role in the dynamics of protein folding or stabilization of protein secondary structures in biological systems. In last few years, several experimental and theoretical works have been performed to investigate the H-bonded interaction of GLY with water molecule.[11,58–67] However, very few studies have been reported on the noncovalent interactions of GLY with itself[7,9,68–70] or with molecules other than water like HCN[4] and THF.[71]

In the present study, we use different quantum chemical models to calculate several intramolecular and intermolecular SSCCs for the isolated GLY molecule and its H-bonded clusters, containing up to three monomers in gas-phase. The main objective of this work is to observe the effect of hydrogen bond formation on SSCCs, choosing a suitable basis set that offers best compromise between cost and precision. Although some elaborate calculations on the trans-hydrogen-bond coupling constants for peptide molecular systems have been performed recently,[28,29,32] no such calculations on glycine cluster has been reported yet. Conversely, gas-phase NMR measurements are also limited to small molecular systems due to the inherent difficulties to perform such experiments.[72] In this context, the present study is important as it may provide some new information regarding the effect of H-bond formation on the SSCCs of —COOH group containing molecules.

2 | METHODS

The most stable gas-phase conformation of isolated GLY molecule is fully optimized without any constraint using the gradient corrected B3LYP (three parameter hybrid exchange functional of Becke with the Lee–Yang–Parr correlation) density functional[73–76] with Pople's 6–31++G(d, p) split-valence basis sets.[77–79] This optimized GLY is considered as the monomer to build the initial structures of H-bonded glycine dimer (GLY···GLY) and trimer (GLY···GLY···GLY) which are then optimized individually by the same model, B3LYP/6–31++G(d,p) with no constraints. Each optimization is followed by the computation of analytical vibrational frequencies at the same level of calculation to confirm that each optimized configuration is a local energy minimum at the potential energy hypersurface. Construction of the initial molecular structures and postcalculation structural analysis are done with molecular structure visualization softwares, ArgusLab[80] and Gaussview 4.1.[81] All the calculations for geometry optimizations and vibrational frequency are performed by using the Gaussian 03 suite of program.[82]

The SSCCs for isolated GLY monomer are then calculated by using the following quantum-chemical models with the geometry optimized at the B3LYP/6–31++G(d,p) level:

SOPPA/aug-cc-pVTZ-J//B3LYP/6–31++G(d,p)
SOPPA(CCSD)/aug-cc-pVTZ-J//B3LYP/6–31++G(d,p)
B3LYP/aug-cc-pVTZ//B3LYP/6–31++G(d,p)
B3LYP/aug-cc-pVTZ-J//B3LYP/6–31++G(d,p)
B3LYP/aug-pcJ-*n* ($n = 0,3$)//B3LYP/6–31++G(d,p)
KT3/aug-cc-pVTZ-J//B3LYP/6–31++G(d,p)
KT3/aug-pcJ-*n* ($n = 0,3$)//B3LYP/6–31++G(d,p)

In all above cases, the model "B3LYP/6–31++G(d,p)" after the "//" symbol denotes the quantum chemical model for geometry optimization and the model before "//" is the one used for the NMR calculations. We could not successfully use the aug-pc-4 basis for the infrastructural limitation. The aug-pc-4 basis for GLY, with 1165 contracted basis functions, is far too expensive compared to the aug-cc-pVTZ-J basis that contains 330 basis functions for the same molecule.

The second-order polarization propagator approximation, SOPPA is based on second-order Møller–Plesset (MP2)[83,84] perturbation theory considering the corresponding singlet or triplet double excitations added to single excitations considered at the level of the random phase approximation (RPA).[85–87] Replacement of the MP2 correlation coefficient in the SOPPA equations with the coupled cluster single and double (CCSD)

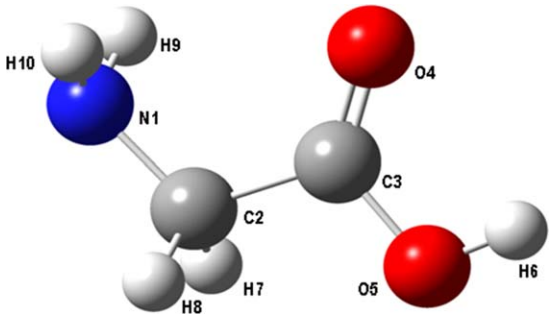

FIGURE 1 The B3LYP/6–31++G(d,p) optimized structure of isolated glycine

excitation amplitudes yields the SOPPA(CCSD) scheme.[88] Hence, both methods consider the electron correlation effects which are important for the coupling among the electronegative atoms. SOPPA has been found to produce very reliable one-bond and long-range spin–spin coupling constants not only in small molecules, but also in a wide range of hydrocarbons.[89] SOPPA(CCSD) results have been considered as the benchmark for the present work.

Among the DFT-based models, B3LYP is one of the most popular hybrid functional which has already been employed successfully in many different types of quantum-chemical investigations over the years. KT3,[90] conversely, belongs to the group of general gradient approximation exchange-correlation (GGA *xc*) functionals, which has been designed specifically to provide high quality NMR shielding constants and chemical shifts. Three different extended basis sets have been used to calculate the SSCCs: (i) the diffuse function augmented correlation consistent aug-cc-pVTZ basis of Dunning and coworkers,[91–93] (ii) the diffuse function augmented spin–spin optimized polarization consistent aug-pcJ-*n* ($n = 0$–4) basis of Jensen,[94,95] and (iii) the diffuse function augmented contracted correlation-consistent triply split polarized aug-cc-pVTZ-J basis of Sauer and coworkers.[96] The last one, in particular, permits an adequate treatment of the cusp of the wave function at the nucleus and, therefore, gives a very good description of the FC term.[97] The aug-cc-pVTZ-J basis is optimized for the calculation of NMR indirect nuclear spin–spin coupling constants with either correlated wavefunction methods such as SOPPA and SOPPA(CCSD) or DFT methods. Results obtained by previous applications of this basis set with different methods were found to be in very good agreement with experiment and it serves as an excellent alternative to calculate SSCCs in large molecules, particularly with B3LYP functional.[97,98]

The calculations with SOPPA and DFT/KT3 functional are performed with the Dalton 16 program package[99] while those with B3LYP are done with Gaussian 09[100] suit of programs. Pople's and Dunning's basis sets are implemented in Gaussian. Sauer's and Jensen's basis set is available from the EMSL basis set library.[101,102]

Besides the glycine monomer, the SSCC parameters for the dimer (GLY···GLY) and trimer (GLY···GLY···GLY) are also calculated, however, only with DFT functionals with aug-cc-pVTZ-J and aug-pcJ-*n*, ($n = 0,1$) basis sets only. Calculation with SOPPA becomes prohibitive for this systems with our current computational infrastructure. The aug-pcJ-*n* basis sets with $n > 2$ are also found to be too costly for dimer and trimer.

In this work, we calculate the one bond ^{1}J (A-B), two bond ^{2}J (A,B) as well as the one-bond ^{1h}J(H···Y) and two-bond ^{2h}J(X,Y) coupling constants across the X—H···Y hydrogen bond to investigate the effect of the hydrogen bond formation where A, B represent any constituent atom of GLY and X, Y are the nonhydrogen atoms. Besides total indirect spin–spin coupling constants, all the individual terms that contribute to the SSCCs, according to Ramsey approach,[103] namely, the Fermi contact (FC), spin dipole (SD), paramagnetic spin-orbit (PSO), and diamagnetic spin-orbit (DSO) have been evaluated for GLY and its H-bonded complexes. The FC and SD terms account for the transmission mechanisms of the spin interaction between nucleus and electrons, while the PSO and DSO contributions treat the interaction between nuclear spins and the orbital angular momentum of the electrons.

3 | RESULTS AND DISCUSSIONS

3.1 | Intramolecular SSCCs—isolated glycine

Glycine in gas-phase, as confirmed by experimental and theoretical investigations,[58,63,104–110] exists predominantly in the neutral form (NH_2CH_2COOH). However, it possesses many different conformations due to the internal rotational degrees of freedom associated with the C—C, C—N, and C—O bonds and possible formation of intramolecular H-bond. The optimized structure of the glycine molecule used in the present work, as shown in Figure 1, corresponds to the most stable and abundant Cs conformations,[105] obtained earlier by ab initio calculations[4,7,58,68,71] and identified experimentally.[63,107–109]

Since the structural parameters of this conformation have already been discussed in details in an earlier publication,[66] we focus our attention directly on the SSCC parameters, the main subject of interest of the present work. Table 1 presents all the intramolecular total one-bond SSCCs, ^{1}J (X,Y) for isolated glycine obtained by different models, as aforementioned.

TABLE 1 One-bond spin–spin coupling constants (in Hz) in the isolated glycine, $^{1}J(X,Y)$, with X,Y = C, N, O, or H, calculated by different models

Method	Basis	$^{15}N_1$—$^{13}C_2$	$^{13}C_2$—$^{13}C_3$	$^{13}C_3$—$^{17}O_4$	$^{13}C_3$—$^{17}O_5$	$^{15}N_1$—$^{1}H_9$	$^{13}C_2$—$^{1}H_7$	$^{17}O_5$—$^{1}H_6$
SOPPA	aug-cc-pVTZ-J	−5.22	55.63	30.05	32.49	−69.41	140.25	−87.05
SOPPA(CCSD)	**aug-cc-pVTZ-J**	**−5.24**	**54.60**	**28.69**	**31.11**	**−67.49**	**135.04**	**−84.92**
DFT-B3LYP	6–31++G(2d,2p)	−6.82	89.49	11.60	28.38	−52.47	92.29	−78.08
DFT-B3LYP	aug-cc-pVTZ	1.50	40.20	46.92	44.49	−62.03	122.01	−73.40
DFT-B3LYP	aug-cc-pVTZ-J	−2.65	53.87	32.42	40.57	−69.71	144.35	−76.58
DFT-B3LYP	aug-pcJ-0	1.11	40.33	50.01	46.97	−56.28	127.69	−49.19
	aug-pcJ-1	−3.97	55.20	29.75	38.28	−68.71	142.45	−76.27
	aug-pcJ-2	−2.80	53.22	32.15	40.10	−69.17	142.89	−76.42
	aug-pcJ-3	−2.79	53.68	32.39	40.48	−69.82	144.03	−77.22
DFT-KT3	aug-cc-pVTZ-J	0.56	46.57	39.05	46.93	−71.99	154.36	−71.89
DFT-KT3	aug-pcJ-0	4.58	33.13	54.26	52.01	−55.81	136.26	−40.97
	aug-pcJ-1	1.32	42.35	40.12	46.02	−66.53	145.08	−64.61
	aug-pcJ-2	2.18	40.91	41.99	47.60	−67.57	146.26	−65.67
	aug-pcJ-3	1.25	44.13	40.71	47.49	−70.36	151.16	−69.84

Comparing the ^{1}J (X,Y) values of different models with that of benchmark SOPPA(CCSD), reported in Table 1, we observe that the DFT/B3LYP functional, either with aug-cc-pVTZ-J or with aug-pcJ-*n* (*n* = 1–3) basis, performs better than KT3 . Among the basis sets, curiously, the double-zeta aug-pcJ-1 is the one that possesses least deviation from SOPPA (CCSD) and performs slightly better than its higher-order family members, aug-pcJ-2 or aug-pcJ-3, as can be seen from Figure 2. In Figure 2, we compare the performance of some of the methods, utilized in the present work, in terms of deviation from SOPPA(CCSD), as defined in the figure itself. The basis sets with triple-zeta quality (aug-cc-pVTZ-J and aug-pcJ-2), conversely, provide similar results for ^{1}J (X,Y) values. However, aug-cc-PVTZ-J works at a lower computational cost. Going from aug-pcJ-2 to aug-pcJ-3, we do not observe significant variation in the ^{1}J (X,Y) values, as can be seen in Table 1, but the computational cost increases manifold. There are a few specific cases in other models, where we observe an excellent agreement. For example, at the KT3/aug-pc-1 level of calculation, $^{1}J(^{15}N_1—^{1}H_9) = -67.57$ Hz, while at the SOPPA(CCSD) level, it is −67.49. The calculated values of $^{1}J(^{15}N_1—^{13}C_2) = -6.82$ Hz, $^{1}J(^{13}C_3—^{17}O_5) = 28.38$ Hz and $^{1}J(^{17}O_5—^{1}H_6) = 78.08$ Hz by B3LYP/6–31++G(2d,2p) are also close to the corresponding SOPPA(CCSD) results. However, considering the factors of computational cost, quality of the basis set and the overall agreement in case of the one-bond interactions in glycine, the performance of aug-cc-pVTZ-J is by far the best one.

We further observe, in Table 1, that the ^{1}J(X, H) absolute values are, in general, higher than those of ^{1}J(X, Y) in all models, where X, Y denote the nonhydrogen atoms of GLY. Among all the interactions, $^{1}J(^{13}C_2—^{1}H_7)$ coupling constants possess highest absolute values, while the ^{1}J

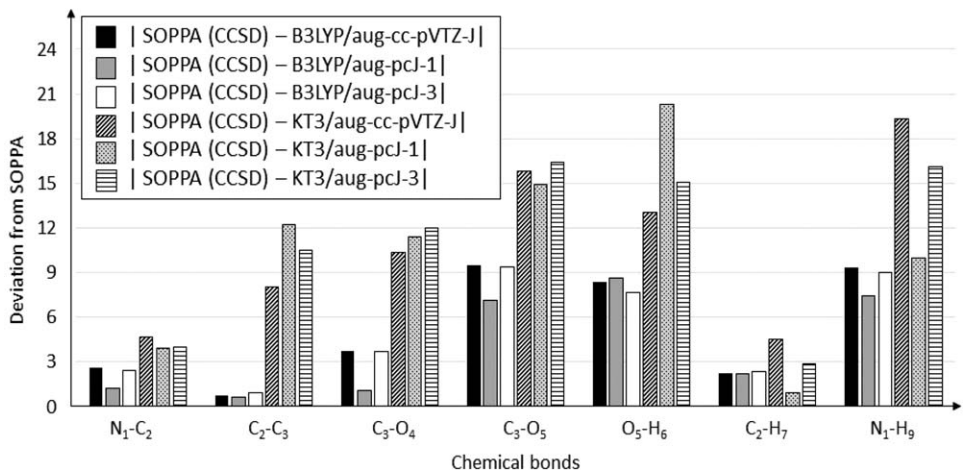

FIGURE 2 Deviations in the $^{1}J(X,Y)$ values when compared with SOPPA(CCSD), as explained in the text

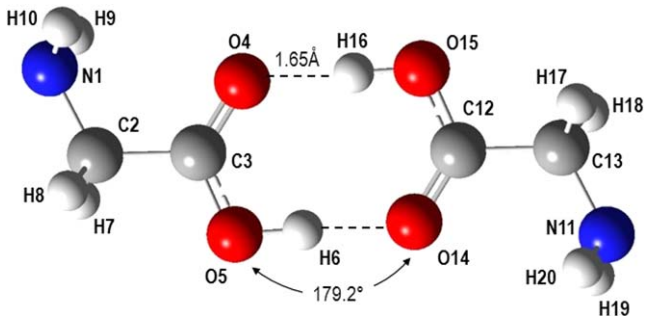

FIGURE 3 B3LYP/6–31++G(d,p) optimized structure of the glycine dimer

($^{15}N_1$—$^{13}C_2$) values are the lowest ones. Thus, both the highest and lowest interaction constants involve the alpha-carbon (C^{α}) of glycine. Among the interactions between the nonhydrogen atoms, the highest value is observed for $^{1}J(^{13}C_2$—$^{13}C_3)$—again involving the same C^{α} atom.

3.2 | Effect of H-bonding on the intramolecular and intermolecular SSCCs

In Figure 3, we show the equilibrium structure H-bonded GLY dimer, GLY···GLY, utilized in the present work. Although the dimer, may contain several conformations due to multiple H-bond sites of GLY, the one containing double H-bonding through the carboxyl group, as shown in Figure 3, is the most stable one in gas-phase.[11] The Figure 4 shows the optimized geometry of the GLY trimer, GLY···GLY···GLY.

The optimized geometry of GLY···GLY is a centro-symmetric structure where two H-bonded carboxyl groups lie in a plane. However, the H-bonded GLY trimer is slightly different. It forms a closed cyclic structure, as shown in Figure 4, where again the main noncovalent stabilizing interactions reside among the three carboxyl groups that do not form a perfect planar structure. The two H-bonds of the dimer are equal, at both length and angle. The trimer, conversely, contains three H-bonds, where the H-bond lengths are almost equal to each other, but the angles are not. The H-bond O···H distances and O—H···O angles are shown in the figures.

Since the H-bonded interactions among the carboxyl group atoms are mainly responsible for the stabilization of the GLY clusters, we attempted to observe the effect of H-bonding on the short-range (one-bond) and long-range (two- and three-bond) SSCCs of these elements in the GLY monomer. In Table 2, we report some of these intramolecular and intermolecular SSCCs as obtained by the models B3LYP/aug-cc-pVTZ-J and B3LYP/aug-pcJ-1. Due to the high computational cost, the calculations of SSCCs for dimer and trimer with the aug-pcJ-2 and aug-pcJ-3 basis became prohibitive in our available infrastructure. Thus, the column called "monomer" in the table shows the values of intramolecular SSCCs when GLY is isolated, some of which have already been reported in Table 1. The columns named "dimer" and "trimer" actually show the modified values of the same monomer SSCCs, when GLY is no longer isolated, but H-bonded with another one or two GLY molecules. The cases where we observe appreciable changes, the numbers are written in bold fonts. The last two lines of Table 2 show the intermolecular or across the H-bonding SSCCs.

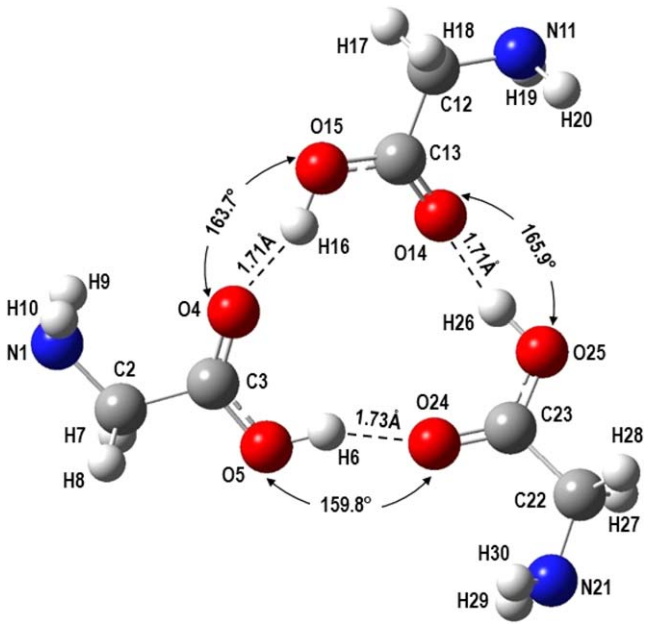

FIGURE 4 B3LYP/6–31++G(d,p) optimized structure of the glycine trimer

TABLE 2 Effect of hydrogen bond formation on SSCCs—variation of intramolecular SSCCs of the glycine monomer 1 when dimer and trimer is formed

	B3LYP/aug-cc-pVTZ-J			B3LYP/aug-pcJ-1		
	Monomer	Dimer	Trimer	Monomer	Dimer	Trimer
No of basis functions	330	660	990	250	500	750
Intramolecular SSCCs (in Hz)						
$^{1}J(C_2—C_3)$	53.87	53.48	54.32	55.20	54.45	55.36
$^{1}J(C_3—O_4)$	32.42	32.99	**30.06**	29.75	30.50	**27.35**
$^{1}J(C_3—O_5)$	40.57	**37.60**	37.34	38.28	**35.46**	35.22
$^{1}J(O_5—H_6)$	−76.58	**–80.57**	**–87.81**	−76.27	**–79.33**	**–86.56**
$^{2}J(C_2—O_4)$	−1.71	**–3.89**	−3.58	−1.57	**–3.69**	−3.36
$^{2}J(C_2—O_5)$	−21.27	**–17.52**	**–19.85**	−20.26	**–16.61**	**–18.84**
$^{2}J(O_4—O_5)$	−6.99	−7.94	−7.32	−7.11	−8.06	−7.43
$^{2}J(C_3—H_6)$	−6.44	−5.84	−5.68	−6.51	−5.93	−5.80
$^{3}J(C_2—H_6)$	7.96	7.78	**8.71**	7.70	7.52	**8.41**
$^{3}J(O_4—H_6)$	1.97	**0.34**	**0.90**	1.95	**0.45**	**1.00**
Intermolecular (across the H-bond) SSCCs (in Hz)						
$^{1h}J(O_4,H_{16})^a$	—	8.00	9.70	—	7.83	9.45
$^{2h}J(O_4,O_{15})^a$	—	6.57	8.53	—	6.28	8.15

[a]For dimer, $^{1h}J(O_4,H_{16}) = {}^{1h}J(O_{14},H_6)$ and $^{2h}J(O_5,O_{14}) = {}^{2h}J(O_4,O_{15})$, by symmetry

In the case of intramolecular interactions, as we observe in Table 2, the changes in the SSCCs involving the interaction of the proton-acceptor oxygen (O_4) atom are higher than those involving the proton-donor oxygen (O_5), when H-bond is formed. For example, the computed value of $^{1}J(O_5—H_6)$ changes from −76.58 Hz to −80.57 Hz when the dimer is formed, which means a variation of about 5% with respect to the monomer value at the B3LYP/aug-cc-pVTZ-J level of calculation. When the trimer is formed, the variation corresponds to about 15% of the monomer value. In the case of the two-bond interaction between the alpha-carbon, C_2 and the proton-donor O_5, $^{2}J(C_2—O_5) = -21.27$ Hz for monomer, but −17.52 Hz for dimer that signifies a variation of about 18% with respect to monomer. Conversely, the calculated value of two-bond, $^{2}J(C_2—O_4)$ changes from 1.97 Hz (monomer) to 0.34 Hz (dimer) to 0.90 Hz (trimer)—a variation of 83% when dimer is formed and 54% when trimer is formed. The B3LYP/aug-pcJ-1 values also demonstrate very similar trend in all cases.

In the context of the present work, it might be interesting to observe the effect of H-bonding on the $^{17}O—^{17}O$ interactions with special care. It is well known that oxygen is one of the most important elements in biomolecular systems. Among all the naturally occurring oxygen isotopes, ^{17}O is the only one that possesses nonzero nuclear spin ($I = 5/2$). However, it has extremely low natural abundance (∼0.037%). Moreover, the nuclear spin $I = 5/2$ implies a nonzero nuclear electric quadrupole moment which tends to cause the broadening of the NMR line widths making the experimental detection of ^{17}O NMR signal somewhat difficult. This increases the importance of high-level theoretical investigations on the magnetic properties of oxygen atoms in biological molecules. When the interaction between the two oxygen nuclei of the carboxyl group in isolated GLY molecule, is considered, as we see in Table 2, $^{2}J(O_4—O_5) = -6.99$ (−7.11) Hz at the B3LYP/aug-cc-pVTZ-J (B3LYP/aug-pcJ-1) level of calculation. With the formation of H-bonds in dimer, the value of the same intramolecular two-bond SSCC changes to −7.94 (−8.06) Hz—an appreciable variation of about 14% (13%) at the B3LYP/aug-cc-pVTZ-J (B3LYP/aug-pcJ-1) level. Going from dimer to trimer, the absolute value of the intramolecular $^{2}J(O_4—O_5)$ SSCC decreases about 7% with respect to its dimer value, in both models.

As far as the intermolecular $^{17}O—^{17}O$ interactions are concerned, we find, in case of the dimer, $^{2h}J(O_4,O_{15}) = {}^{2h}J(O_{14},O_5) = 6.57$ (6.28) Hz at the B3LYP/aug-cc-pVTZ-J (B3LYP/aug-pcJ-1) level of calculation which jumps to 8.53 (8.15) Hz when the trimer is formed. Once again, an appreciable effect of H-bonded interaction on the magnetic properties of oxygen is observed with a variation of about 30% at both levels. We note that the sign of the intramolecular $^{2}J(O_4,O_5)$ is negative, while that of the intermolecular $^{2h}J(O_4,O_{15})$ is positive. Furthermore, the sign of the intramolecular one-bond SSCC of the proton donor O—H group $^{1}J(O_5—H_6)$ is negative while that of the across the H-bond SSCC $^{1h}J(O_4—H_{16})$ is positive. Since the gyromagnetic ratio of ^{17}O is negative and that of ^{1}H is positive, the reduced intramolecular (through-bond) SSCC, $^{1}K(O_5,H_6)$ is positive and $^{2}K(O_4,O_5)$ is negative, in agreement with the predictions of Dirac Vector Model (DVM). Likewise, The reduced intermolecular (across the H-bond) SSCC $^{1h}K(O_5,H_6)$ is negative and $^{2h}K(O_4,O_5)$ is positive, consistent with the nuclear magnetic resonance triplet Wave function model (NMRTWM).[111,112] The $^{1h}J(O_4—H_{16})$ also suffers appreciable variation (more than 20%) at both B3LYP and KT3 levels, while going from dimer to trimer.

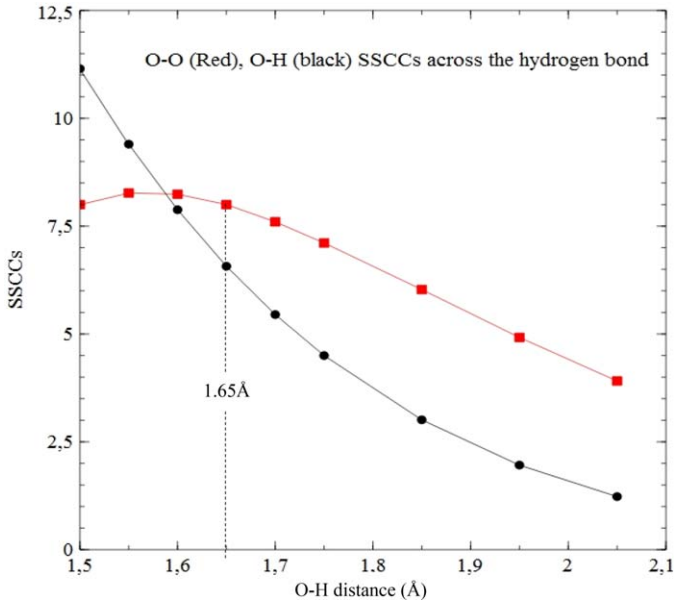

FIGURE 5 Variation of O—H and O—O SSCC as a function of Hydrogen bond length

In Figure 5, we illustrate the variation of intermolecular, or, "across the H-bond" $^{17}O—^{17}O$ and $^{17}O—^{1}H$ SSCC as a function of the proton-transfer coordinate in Gly dimer. As we observe from the figure, $^{1h}J(^{17}O—^{1}H)$ just decreases monotonously as the O—H distance increases. Conversely, $^{2h}J(^{17}O—^{17}O)$ shows slight increase in between 1.55 and 1.60 Å and then starts to decrease and beyond 1.65Å, which is the H-bond length of the dimer equilibrium geometry, it also decreases gradually. If we observe the three H-bond angles in trimer, as illustrated in Figure 4, they can be arranged in the following order: $\theta(O_6—H_5\cdots O_{24}) = 159.8° < \theta(O_4—H_{16}\cdots O_{15}) = 163.7° < \theta(O_{14}—H_{26}\cdots O_{25}) = 165.9°$. The corresponding $^{2h}J(^{17}O—^{17}O)$ values maintain a different order, which is, $^{2h}J(O_6—O_{24}) = 8.51$ Hz $< {}^{2h}J(O_4—O_{15}) = 8.53$ Hz $> {}^{2h}J(O_{14}—O_{25}) = 7.74$ Hz, as calculated by B3LYP/aug-cc-pVTZ-J model. Thus, no special correlation is found between SSCC values and H-bond lengths or H-bond angles.

In Table 3, we report the values of individual Ramsey terms to analyze their relative contributions to total SSCC. In many systems, the FC term is found to be the most dominant among the four. However, in the present case, where the carboxyl group atoms are being analyzed, this is not always true. In some cases like, $^{1}J(C_3—O_5)$, $^{1}J(O_5—H_6)$, or $^{2}J(C_2—O_5)$, FC term is the highest contributor to SSCC values followed by the paramagnetic spin-orbit (PSO) and its value is always more than an order of magnitude larger than any other Ramsey terms. Conversely, there are other interactions, where the contribution of PSO term surpasses that of FC term, as observed before in case of microhydrated ortho-aminobenzoic acid.[23] For example, in $^{2}J(O_4—O_5)$ and $^{3}J(O_4—H_6)$ the PSO term is found to be stronger than FC by one order of magnitude. It is to be noted that both of these interactions involve O_4, the proton-acceptor oxygen of the carboxyl group. In fact, there are situations where the FC term is dominant even though O_4 is present in the interaction, like $^{1}J(C_3—O_4)$ or $^{2}J(C_2—O_4)$. But, the dominance of FC term is less expressive in these cases, as both FC and PSO are of same order of magnitude. For example, in $^{1}J(C_3—O_4)$ of GLY monomer, while the FC term is 21.22 (18.40) Hz at the B3LYP/aug-cc-pVTZ-J (B3LYP/aug-pcJ-1) level of calculation, the corresponding PSO term is 13.59 (14.08) Hz. Thus, individual Ramsey terms are sensitive to the particular function of oxygen atom when H-bonding takes place. In general, the dominance of FC term is valid for all one-bond SSCCs. The few cases where PSO contributes more than FC belong to two- or higher-bond SSCCs.

Regarding the effect of H-bonded interactions, we again observe an appreciable influence, although no particular pattern is noted. The one-bond $^{17}O—^{1}H$ interaction shows most notable variations among all. The FC term of $^{1}J(O_5—H_6)$ changes from −66.73 Hz in isolated GLY to −75.37 Hz when dimer is formed (signifying a variation of ca. 13%) and −81.65 Hz when trimer is formed (variation of 22% with respect to isolated monomer) at the B3LYP/aug-cc-pVTZ-J level of calculation. The B3LYP/aug-pcJ-1 model predicts similar variations. Unlike the FC terms, the absolute value of PSO in $^{1}J(O_5—H_6)$ decreases by about 47% with dimer formation and 38% with trimer formation at both level of calculation. Among other one-bond interactions, the FC term of $^{1}J(C_3—O_4)$ suffers almost no variation when dimer is formed, but decreases by about 12% with trimer formation. The value of the PSO term remains around 13 (14) Hz in all systems at the B3LYP/aug-cc-pVTZ-J (B3LYP/aug-pcJ-1) level of calculation. On the contrary, the FC term of $^{1}J(C_3—O_5)$ suffers variation when dimer is formed with a diminution of about 15% (16%), at the B3LYP/aug-cc-pVTZ-J (B3LYP/aug-pcJ-1) level of calculation but remained almost unchanged when going from dimer to trimer. In this last case, however, the variation of the PSO term follows an opposite trend—it increases by about 30% (27%) at the same levels of calculation, when dimer is formed and then remains almost unaltered.

TABLE 3 Calculated values of the individual Ramsey terms (in units of Hz) of isolated and hydrogen-bonded glycine using two diferente quantum–chemical models: B3LYP/aug-cc-pVTZ-J and KT3/aug-cc-pVTZ-J

		B3LYP/aug-cc-pVTZ-J			B3LYP/aug-pcJ-1		
Coupling	RP	Monomer	Dimer	Trimer	Monomer	Dimer	Trimer
$^{1}J(C_3—O_4)$	DSO	−0.10	−0.13	−0.13	−0.10	−0.13	−0.13
	PSO	13.59	13.32	12.99	14.08	13.79	13.46
	SD	−2.32	−1.29	−1.50	−2.63	−1.51	−1.74
	FC	21.22	21.07	18.66	18.40	18.35	15.75
$^{1}J(C_3—O_5)$	DSO	−0.14	−0.15	−0.15	−0.14	−0.15	−0.15
	PSO	6.74	8.74	8.31	6.96	9.04	8.59
	SD	0.11	0.20	0.18	0.07	0.15	0.13
	FC	33.84	28.80	28.99	31.39	26.42	26.66
$^{1}J(O_5—H_6)$	DSO	−0.33	−0.53	−0.51	−0.33	−0.53	−0.51
	PSO	−9.56	−5.03	−5.92	−9.73	−5.12	−6.02
	SD	0.02	0.33	0.24	−0.23	0.09	−0.02
	FC	−66.73	−75.37	−81.65	−65.98	−73.77	−80.02
$^{2}J(C_2—O_4)$	DSO	0.03	0.02	0.02	0.03	0.02	0.02
	PSO	1.19	1.09	1.11	1.23	1.13	1.15
	SD	−0.20	−0.16	−0.17	−0.20	−0.15	−0.17
	FC	−2.73	−4.84	−4.54	−2.63	−4.67	−4.35
$^{2}J(C_2—O_5)$	DSO	−0.01	−0.01	−0.01	−0.01	−0.01	−0.01
	PSO	0.34	0.58	0.50	0.36	0.59	0.52
	SD	0.04	0.01	0.02	0.05	0.01	0.02
	FC	−21.68	−18.11	−20.38	−20.66	−17.20	−19.36
$^{2}J(O_4—O_5)$	DSO	−0.04	−0.03	−0.03	−0.04	−0.03	−0.03
	PSO	−6.86	−7.29	−6.88	−7.12	−7.55	−7.13
	SD	0.82	0.91	0.91	0.88	0.97	0.98
	FC	−0.91	−1.52	−1.33	−0.84	−1.46	−1.25
$^{2}J(C_3—H_6)$	DSO	−0.43	−0.28	−0.39	−0.43	−0.29	−0.39
	PSO	−1.08	−1.26	−1.08	−1.17	−1.34	−1.16
	SD	−0.15	−0.17	−0.17	−0.16	−0.19	−0.19
	FC	−4.79	−4.13	−4.04	−4.75	−4.10	−4.06
$^{3}J(C_2—H_6)$	DSO	−0.72	−0.58	−0.60	−0.72	−0.58	−0.61
	PSO	0.61	0.56	0.58	0.61	0.57	0.58
	SD	0.04	0.06	0.05	0.04	0.06	0.05
	FC	8.03	7.75	8.69	7.77	7.48	8.38
$^{3}J(O_4—H_6)$	DSO	0.02	−0.07	−0.05	0.02	−0.07	−0.05
	PSO	2.30	1.74	1.90	2.34	1.76	1.93
	SD	0.48	0.38	0.38	0.51	0.41	0.40
	FC	−0.83	−1.71	−1.32	−0.82	−1.65	−1.29

TABLE 4 The effect of structural modifications and electronic interactions on SSCCs (in Hz) as calculated by the B3LYP/aug-cc-pVTZ-J model

			Constrained GLY with interaction		Constrained GLY without interaction	
Coupling	RP	Relaxed GLY	Dimer	Trimer	Dimer	Trimer
$^{1}J(C_3—O_4)$	DSO	−0.10	−0.13	−0.13	−0.11	−0.10
	PSO	13.59	13.32	12.99	14.06	13.90
	SD	−2.32	−1.29	−1.50	−2.21	−2.23
	FC	21.22	21.07	18.66	24.96	23.64
	Total	**32.42**	**32.99**	**30.06**	**36.70**	**35.21**
$^{1}J(C_3—O_5)$	DSO	−0.14	−0.15	−0.15	−0.14	−0.14
	PSO	6.74	8.74	8.31	7.05	6.82
	SD	0.11	0.20	0.18	0.28	0.27
	FC	33.84	28.80	28.99	31.01	31.32
	Total	**40.57**	**37.60**	**37.34**	**38.20**	**38.28**
$^{1}J(O_5—H_6)$	DSO	−0.33	−0.53	−0.51	−0.34	−0.35
	PSO	−9.56	−5.03	−5.92	−9.19	−9.41
	SD	0.02	0.33	0.24	0.31	0.14
	FC	−66.73	−75.37	−81.65	−61.21	−67.22
	Total	**−76.58**	**−80.57**	**−87.81**	**−70.43**	**−76.84**
$^{2}J(O_4—O_5)$	DSO	−0.04	−0.03	−0.03	−0.04	−0.04
	PSO	−6.86	−7.29	−6.88	−6.52	−6.46
	SD	0.82	0.91	0.91	1.03	0.97
	FC	−0.91	−1.52	−1.33	−0.76	−0.76
	Total	**−6.99**	**−7.94**	**−7.32**	**−6.29**	**−6.29**
$^{3}J(O_4—H_6)$	DSO	0.02	−0.07	−0.05	0.05	−0.08
	PSO	2.30	1.74	1.90	2.13	2.10
	SD	0.48	0.38	0.38	0.45	0.42
	FC	−0.83	−1.71	−1.32	−0.79	−0.84
	Total	**1.97**	**0.34**	**0.90**	**1.84**	**1.77**

3.3 | Factors controlling the variation of SSCCs

The formation of molecular clusters, in gas phase, may be interpreted as a two-step process.[7,113,114] In the first step, the monomers approach each other, make necessary adjustment in their geometries, and align themselves appropriately so that, in the next step, the intermolecular electronic interactions (electrostatic, polarization, exchange, charge transfer, etc.) may effectively be established giving necessary stability to the clusters. The SSCCs of the monomer can thus be influenced by two factors—the structural modification and the electronic interaction and there may exist a competition between them. In the present section, we make a brief analysis of the effect of these two factors on the calculated SSCCs of glycine. We thus consider two different kinds of monomer geometry in the case of homogeneous glycine cluster. First, we have the constraint-free equilibrium geometry of the glycine molecule, which we call as "relaxed GLY" in the present discussion. Second, there is the geometry adopted inside the clusters, which is slightly distorted with respect to the original equilibrium geometry, and we name it as "constrained GLY." Inside the cluster (dimer or trimer), this "constrained GLY" interacts with another "constrained GLY" through H-bonding. Thus, the SSCCs calculated in a cluster include the effect of both factors—the structural modification and the electronic interaction, However, if we extract the constrained monomer from the cluster and calculate SSCCs on this geometry separately, we can observe the sole effect of structural modification. So, the "constrained GLY" is further classified as "constrained GLY with interaction" and "constrained GLY without interaction." In Table 4, we report the SSCCs of the GLY monomer in these three different situations and observe their relative importance in the variation of the SSCCs.

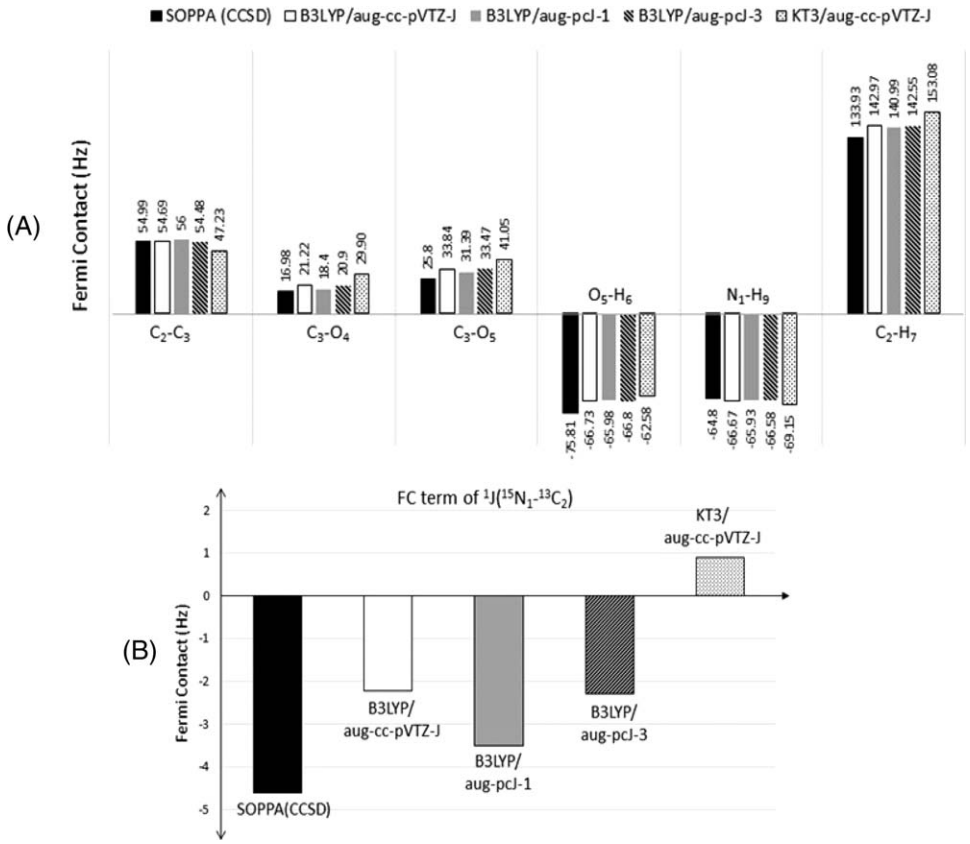

FIGURE 6 A, The Fermi-contact (FC) terms for various one-bond nuclear interactions in isolated glycine molecules calculated by using different DFT models and SOPPA methodology. B, FC terms for one-bond $^{15}N—^{13}C$ only by same methods

For the $^{1}J(C_3—O_4)$, both in dimer and trimer, the influences run in opposite directions, while structural modification increases the SSCC, H-bonded interaction decreases it. In case of the dimer, the effect of electronic interaction cannot overcome the effect of structural modification and, as a result, we have a net increase of 0.6 Hz in "constrained GLY with interaction." In case of the trimer, we observe an increase of about 2.8 Hz in the total SSCC of the "constrained GLY without interaction" with respect to that of "relaxed GLY." Thus, the structural modifications affect the $^{1}J(C_3—O_4)$ appreciably. However, the electronic interaction turns out to be even more important in this case as it not only nullifies the increase of this SSCC due to structural changes, it decreases it almost by the same amount, giving a net decrease of 2.4 Hz in "constrained GLY with interaction."

In the case of $^{1}J(C_3—O_5)$, conversely, the influences of geometry and interaction run in the same direction, both in dimer and trimer. The values of $^{1}J(C_3—O_5)$ decrease in all cases. However, in case of dimer, the effect of electronic interaction overcomes the effect of structural modification and causes more decrease in $^{1}J(C_3—O_5)$. As we can observe from Table 4, the total values of this SSCC for the "constrained GLY without interaction" and "constrained GLY with interaction" are 2.37 Hz and 2.97 Hz, respectively. Thus, going from monomer to dimer, there is a decrease of 2.4 Hz in $^{1}J(C_3—O_5)$ just due to geometrical changes and when the electronic interaction comes into play, it decreases the $^{1}J(C_3—O_5)$ further by 0.6 Hz. In the trimer, the same behavior is observed. However, the decrease in $^{1}J(C_3—O_5)$ solely due to electronic interaction is just 0.9 Hz. Thus, in case of $^{1}J(C_3—O_5)$, it is the structural modifications that plays a dominant role in the variation of SSCC.

The $^{1}J(O_5—H_6)$ coupling constants show larger variations, in both dimer and trimer, as expected. In dimer, the influences of geometry and interaction run in opposite direction. While structural modification increases the $^{1}J(O_5—H_6)$ by 6.15 Hz, the joint effect of geometric modification and H-bonding interaction decreases it by 3.99 Hz, when compared with the same SSCC of "relaxed GLY." Thus, the sole effect of electronic interaction is 10.14 Hz, which is appreciable. In case of the trimer, the effect of geometric modification runs in the same direction as the electronic interaction, but the former is insignificant in comparison with the later. The electronic interaction, in this case, alone causes a decrease of 10.97 Hz when the total decrease due to joint effect of geometry and interaction is 11.23 Hz. Therefore, once again the electronic interaction plays major role in the variation of SSCC.

In the same way, for the two-bond and three-bond coupling constants reported in the Table 4, we can observe that the principle factor responsible for the variation of the SSCCs in the monomer is the electronic effect introduced by the neighbors in the cluster through hydrogen bonding.

3.4 | Variation of FC terms in GLY monomer

Since the FC interaction has the dominant contribution to the total one-bond SSCCs among all the Ramsey contributions, it may be appropriate to compare the values of FC terms, for different interactions, obtained by different models with those obtained by the benchmark SOPPA(CCSD) and we have done that in Figure 6. As we can see from Figure 6A, all the models show very similar general trend, although B3LYP shows better agreement with SOPPA than KT3 as far as the numerical values of the SSCCs are concerned. In case of the one-bond $^{1}J(^{15}N—^{13}C)$ interaction, shown separately in Figure 6B, KT3 goes in a different direction – while $^{1}J(^{15}N_1—^{13}C_{2)} = -4.61$ Hz at SOPPA/aug-cc-pVTZ-J, −3.5 Hz at B3LYP/aug-pcJ-1, and −2.22 (–2.29) Hz at the B3LYP/aug-cc-pVTZ-J (B3LYP/aug-pcJ-3) level of calculation, KT3/aug-cc-pVTZ-J computes, $^{1}J(^{15}N_1—^{13}C_{2)} = +0.89$ Hz.

In case of both the "relaxed GLY" and "constrained GLY" with or without interaction, the one-bond SSCCs are dominated by FC contributions followed by PSO with negligible contributions coming from SD and DSO terms, as seen before. The variations of the FC term under the influence of the "structural modifications" and the "electronic interaction" follows the same trend as the total SSCC in case of $^{1}J(O_5—H_6)$ coupling constant. But in other cases, it shows a different personality. For example, in case of $^{1}J(C_3—O_5)$, the influence of electronic interaction in the variation of FC term is as big as structural modification, in both dimer and trimer as can be seen from Table 4. In case of total SSCC it was quite small compared to that of structural modification. In case of $^{1}J(C_3—O_4)$ also the factor of electronic interaction surpasses the structural modification as far their influence on the variation of FC term is concerned, in both dimer and trimer. Moreover, in both clusters, unlike the variation total SSCC the influences of the two factors on FC run in opposite directions.

4 | CONCLUSION

In this work, we make a detailed theoretical study of the effects of hydrogen bond formation on the nuclear spin–spin coupling constants (SSCC) of the glycine molecule in gas-phase. The intermolecular and intramolecular coupling constants of the isolated glycine and hydrogen-bonded homogeneous glycine clusters containing upto three monomers are calculated using different quantum-chemical methods including SOPPA(CCSD) with the geometry optimized at the B3LYP/6–31++G(d,p) level. After benchmarking the SSCC values obtained by different DFT models against those obtained by SOPPA(CCSD), the B3LYP/aug-cc-pVTZ-J model is found to be a suitable choice for SSCC calculations considering its triple zeta quality, computational cost effectiveness, and numerical precision.

The hydrogen-bonded interactions are found to cause significant variations in the one-bond nuclear interactions for the atoms directly participating in the interaction. During the formation of clusters the participating monomers suffer structural modifications to establish the appropriate electronic interactions among themselves. Although both of these factors contribute individually and appreciably in the variation of the nuclear coupling constants, the contribution of electronic interactions is found to be stronger than that of structural modification. Between the two oxygen atoms of glycine (proton-donor and proton acceptor), the effect of H-bonding is more prominent for the one-bond SSCCs involving the proton-donor oxygen. The two-bond across the H-bond SSCC suffers higher variation compared to the one-bond across the H-bond SSCC when the size of the H-bonded cluster increases.

The sign of intramolecular two-bond ($^{17}O,^{17}O$) SSCC is negative, but the intermolecular (across the H-bond) two-bond ($^{17}O,^{17}O$) SSCC is positive. The sign of intramolecular one-bond ($^{17}O,^{1}H$) SSCC is negative while that of the across the H-bond $^{1h}J(^{17}O,^{1}H)$ is positive. These variations of sign of one-bond and two-bond SSCCs are consistent with the predictions of Dirac vector model and nuclear magnetic resonance triplet wave function model. Among the four Ramsey terms that constitute the total SSCC, the FC term is the dominant contributor followed by the PSO term in all one-bond interaction. For two-, three-, and higher order SSCCs, PSO becomes the principal contributor if proton-acceptor oxygen takes part in the interaction. The individual Ramsey terms are also found to be sensitive to the particular function of the oxygen atom (proton-donor or proton-acceptor) in the hydrogen-bonded clusters. In case of the one-bond ($^{13}C,^{17}O$) couplings, the nature of the variation of FC terms as a function of structural modification and electronic interaction is different from that of the total SSCC.

ACKNOWLEDGMENTS

P.C. gratefully acknowledges the financial support from Brazilian funding agency CNPq. P.F.P. acknowledge financial support from CONICET and UNNE (No. PI:15/F002 Res. 1017/15). SC acknowledges CNPq, CAPES, and FAPESP for continuous support.

ORCID

Puspitapallab Chaudhuri http://orcid.org/0000-0001-9748-9890

REFERENCES

[1] A. Sadybekov, A. I. Krylov, *J. Chem. Phys.* **2017**, *147*, 014107.

[2] M. Lingbiao, W. Wu, Z. Lin, *Phys. Chem. Chem. Phys.* **2016**, *18*, 15894.

[3] J. Sun, G. Niehues, H. Forbert, D. Decka, G. Schwaab, D. Marx, M. Havenith, *J. Am. Chem. Soc.* **2014**, *136*, 5031.

[4] A. M. Silva, A. Ghosh, P. Chaudhuri, *J. Phys. Chem. A* **2013**, *117*, 10274.

[5] B. Yogeswari, R. Kanakaraju, S. Boopathi, P. Kolandaivel, *J. Mol. Graph. Model.* **2012**, *35*, 11.

[6] M. D. Ganji, A. Bakhshandeh, *Phys. B Condens. Matter* **2011**, *406*, 4453.

[7] P. Chaudhuri, S. Canuto, *Chem. Phys. Lett.* **2010**, *491*, 86.

[8] B. Brauer, G. M. Chaban, R. B. Gerber, *Phys. Chem. Chem. Phys.* **2004**, *6*, 2543.

[9] J. Chocholoušov, J. Vacek, F. Huisken, O. Werhahn, P. Hobza, *J. Phys. Chem. A* **2002**, *106*, 11540.

[10] Q. Cui, *J. Chem. Phys.* **2002**, *117*, 4720.

[11] P. Bandyopadhyay, M. S. Gordon, *J. Chem. Phys.* **2000**, *113*, 1104.

[12] M. Nyberg, J. Hasselström, O. Karis, N. Wassdahl, M. Weinelt, A. Nilsson, L. G. M. Pettersson, *J. Chem. Phys.* **2000**, *112*, 5420.

[13] R. T. Garrod, *Astrophys. J.* **2013**, *657*, 60.

[14] S. Pilling, L. Baptista, H. M. Boechat-Roberty, D. P. P. Andrade, *Astrobiology* **2011**, *11*, 883.

[15] L. E. Snyder, *Orig. Life Evol. Biosph.* **1997**, *27*, 115.

[16] C. Ceccarelli, L. Loinard, A. Castets, A. Faure, B. Lefloch, *Astron. Astrophys.* **2000**, *362*, 1122.

[17] Y. J. Kuan, S. B. Charnley, H. C. Huang, W.-L. Tseng, Z. Kisiel, *Astrophys. J.* **2003**, *593*, 848.

[18] L. E. Snyder, F. J. Lovas, J. M. Hollis, D. N. Friedel, P. R. Jewell, A. Remijan, V. V. Ilyushin, E. A. Alekseev, S. F. Dyubko, *Astrophys. J.* **2005**, *619*, 914.

[19] K. Altwegg, H. Balsiger, A. Bar-Nun, J.-J. Berthelier, A. Bieler, P. Bochsler, C. Briois, U. Calmonte, M. R. Combi, H. Cottin, J. De Keyser, F. Dhooghe, B. Fiethe, S. A. Fuselier, S. Gasc, T. I. Gombosi, K. C. Hansen, M. Haessig, A. Jäckel, E. Kopp, A. Korth, L. Le Roy, U. Mall, B. Marty, O. Mousis, T. Owen, H. Rème, M. Rubin, T. Sémon, C.-Y. Tzou, J. H. Waite, P. Wurz, *Sci. Adv.* **2016**, *2*, e1600285.

[20] J. E. Elsila, D. P. Glavin, J. P. Dworkin, *Meteorit. Planet. Sci.* **2009**, *44*, 1323.

[21] J. S. Fabián, S. Omar, J. M. G. Veja, *J. Chem. Phys.* **2016**, *145*, 084301.

[22] Y. Y. Rusakov, L. B. Krivdin, *Russ. Chem. Rev.* **2013**, *82*, 99.

[23] A. Ghosh, V. B. Pacheco, P. Chaudhuri, *Mol. Phys.* **2013**, *111*, 403.

[24] P. F. Provasi, M. C. Caputo, S. P. A. Sauer, I. Alkorta, J. Elguero, *Comput. Theor. Chem.* **2012**, *998*, 98.

[25] R. M. Gester, H. C. Georg, S. Canuto, M. C. Caputo, P. F. Provasi, *J. Phys. Chem. A* **2009**, *113*, 14936.

[26] M. Tafazzoli, S. K. Amini, *Magn. Reson. Chem.* **2008**, *46*, 370.

[27] I. Alkorta, J. Elguero, G. S. A. Denisov, *Magn. Reson. Chem.* **2008**, *46*, 599.

[28] P. Salvador, R. Wieczorek, J. J. Dannenberg, *J. Phys. Chem. B* **2007**, *111*, 2398.

[29] T. V. Mourik, A. J. Dingley, *J. Phys. Chem. A* **2007**, *111*, 11350.

[30] L. B. Krivdin, R. H. Contreras, *Annu. Rep. NMR Spectrosc.* **2007**, *61*, 133.

[31] P. F. Provasi, G. A. Aucar, M. Sanchez, I. Alkorta, J. Elguero, S. P. A. Sauer, *J. Phys. Chem. A* **2005**, *109*, 6555.

[32] P. Salvador, N. Kobko, R. Wieczorek, J. J. Dannenberg, *J. Am. Chem. Soc.* **2004**, *126*, 14190

[33] J. E. Del Bene, S. A. Perera, R. J. Bartlett, *J. Phys. Chem. A* **2001**, *105*, 930.

[34] J. E. Del Bene, S. A. Perera, R. J. Bartlett, *J. Am. Chem. Soc.* **2000**, *122*, 3560.

[35] M. Jaszunski, K. Ruud, P. Lantto, J. Vaara, *Chem. Phys. Lett.* **2001**, *114*, 5482.

[36] O. Vahtras, H. Ågren, P. Jørgensen, H. J. A. Jensen, S. B. Padkjær, T. Helgaker, *J. Chem. Phys.* **1992**, *96*, 6120.

[37] T. Helgaker, M. Jaszunski, K. Ruud, A. Gońska, *Theo. Chem. Acc.* **1998**, *99*, 175.

[38] P. Jørgensen, H. Jensen, J. Olsen, *J. Chem. Phys.* **1988**, *89*, 3654.

[39] E. S. Nielsen, P. Jørgensen, J. Oddershede, *J. Chem. Phys.* **1980**, *73*, 6238.

[40] J. Geertsen, P. Jørgensen, *Chem. Phys.* **1984**, *90*, 301.

[41] M. J. Packer, E. K. Dalskov, T. Enevoldsen, H. J. A. Jensen, J. Oddershede, *J. Chem. Phys.* **1996**, *105*, 5886.

[42] T. Enevoldsen, J. Oddershede, S. P. A. Sauer, *Theor. Chem. Acc.* **1998**, *100*, 275.

[43] H. Sekino, R. J. Bartlett, *J. Chem. Phys.* **1986**, *85*, 3945.

[44] S. A. Perera, H. Sekino, R. J. Bartlett, *J. Chem. Phys.* **1994**, *101*, 2186.

[45] S. A. Perera, M. Nooijen, R. J. Bartlett, *J. Chem. Phys.* **1996**, *104*, 3290.

[46] H. Koch, O. Christiansen, P. Jørgensen, A. M. S. Merás, T. Helgaker, *J. Chem. Phys.* **1997**, *106*, 1808.

[47] A. A. Auer, J. Gauss, *J. Chem. Phys.* **2001**, *115*, 1619.

[48] R. Faber, S. P. A. Sauer, J. Gauss, *J. Chem. Theory Comput.* **2017**, *13*, 696.

[49] J. M. G. Vega, J. S. Fabián, *Mol. Phys.* **2015**, *113*, 1924.

[50] J. S. Fabián, J. M. G. Veja, E. S. Fabián, *J. Chem. Theory Comput.* **2014**, *10*, 4938.

[51] P. Pengju Ren, A. Zheng, X. Pan, X. Han, X. Bao, *J. Phys. Chem. C*, **2013**, *117*, 23418.

[52] T. Kupka, M. Nieradka, M. Stachoẃ, T. Pluta, P. Nowak, H. Kjær, J. Kongsted, J. Kaminsky, *J. Phys. Chem. A* **2012**, *116*, 3728.

[53] J. D. Vilcachagua, L. C. Ducati, R. Rittner, R. H. Contreras, C. F. Tormena, *J. Phys. Chem. A* **2012**, *115*, 1272.

[54] T. Bally, T P. R. Rablen, *J. Org. Chem.* **2011**, *76*, 4818.

[55] J. Kongsted, K. Aidas, K. V. Mikkelsen, S. P. A. Sauer, *J. Chem. Theory Comput.* **2008**, *4*, 267.

[56] T. Kupka, *Magn. Reson. Chem.* **2009**, *47*, 674.

[57] T. W. Keal, D. W. Tozer, T. Helgaker, *Chem. Phys. Lett.* **2004**, *391*, 374.

[58] M. K. Ghosh, T. H. Choi, C. H. Choi, *Theor. Chem. Acc.* **2016**, *135*, 103.

[59] S. Coussana, G. Tarczay, *Chem. Phys. Lett.* **2016**, *644*, 189.

[60] L. Kócs, E. E. Najbauer, G. Bazsó, G. Magyarfalvi, G. Tarczay, *J. Phys. Chem. A* **2015**, *119*, 2429.

[61] M. D. L. Oliver, B. M. Christoph, S. H. Thomas, R. C. Lorenz, K. B. Guenther, W. H. Christian, *Chem. Phys.* **2014**, *435*, 21.

[62] J. Niskanen, N. A. Murugan, Z. Rinkevicius, O. Vahtras, C. C. Li, S. Monti, V. Carravetta, H. Ågren, *Phys. Chem. Chem. Phys.* **2013**, *15*, 244.

[63] R. M. Balabin, *J. Phys. Chem. B* **2010**, *114*, 15075.

[64] S. M. Bachrach, *J. Phys. Chem. A* **2008**, *112*, 3722.

[65] C. Aikens, M. Gordon, *J. Am. Chem. Soc.* **2006**, *128*, 12835.

[66] A. Chaudhari, S.-L. Lee, *Chem. Phys.* **2005**, *310*, 281.

[67] P. Selvarengan, P. Kolandaivel, *J. Mol. Struct. THEOCHEM* **2002**, *617*, 99.

[68] J. R. Carvalho, A. M. Silva, A. Ghosh, P. Chaudhuri, *J. Mol. Struct.* **2016**, *1123*, 55.

[69] P. Friant-Michel, M. F. Ruiz-López, *Chemphyschem* **2010**, *11*, 3499.

[70] M. F. Carvalho, R. A. Mosquera, R. A. Rivelino, *Chem. Phys. Lett.* **2007**, *445*, 117.

[71] D. Kaur, G. Chopra, R. Kaur, *Can. J. Chem.* **2017**, *95*, 664.

[72] K. Jackowski, *J. Mol. Struct.* **2006**, *786*, 215.

[73] A. D. Becke, *J. Chem. Phys.* **1993**, *98*, 5648.

[74] C. Lee, W. Yang, R. G. Parr, *Phys. Rev. B* **1988**, *37*, 785.

[75] S. H. Vosko, L. Wilk, M. Nusair, *Can. J. Phys.* **1980**, *58*, 1200.

[76] P. J. Stephens, F. J. Devlin, M. J. Frisch, C. F. Chabalowski, *J. Phys. Chem.* **1994**, *98*, 11623.

[77] W. J. Hehre, R. Ditchfield, J. A. Pople, *J. Chem. Phys.* **1972**, *56*, 2257.

[78] M. M. Francl, W. J. Pietro, W. J. Hehre, J. S. Binkley, D. J. DeFrees, J. A. Pople, M. S. Gordon, *J. Chem. Phys.* **1982**, *77*, 3654.

[79] T. Clark, J. Chandrasekhar, G. W. Spitznagel, P. V. R. Schleyer, *J. Comput. Chem.* **1983**, *4*, 294.

[80] M. A. Thompson, *ArgusLab 4.0.1—Computational Chemistry Software*, Planaria Software LLC, Seattle, WA, **2004**.

[81] R. Dennington, T. Keith, J. Millam, *GaussView, Version 4.1.2*, Semichem Inc., Shawnee Mission, KS **2006**.

[82] M. J. Frisch, G. W. Trucks, H. B. Schlegel, G. E. Scuseria, M. A. Robb, J. R. Cheeseman, J. A. Montgomery, Jr, T. Vreven, K. N. Kudin, J. C. Burant, J. M. Millam, S. S. Iyengar, J. Tomasi, V. Barone, B. Mennucci, M. Cossi, G. Scalmani, N. Rega, G. A. Petersson, H. Nakatsuji, M. Hada, M. Ehara, K. Toyota, R. Fukuda, J. Hasegawa, M. Ishida, T. Nakajima, Y. Honda, O. Kitao, H. Nakai, M. Klene, X. Li, J. E. Knox, H. P. Hratchian, J. B. Cross, V. Bakken, C. Adamo, J. Jaramillo, R. Gomperts, R. E. Stratmann, O. Yazyev, A. J. Austin, R. Cammi, C. Pomelli, J. W. Ochterski, P. Y. Ayala, K. Morokuma, G. A. Voth, P. Salvador, J. J. Dannenberg, V. G. Zakrzewski, S. Dapprich, A. D. Daniels, M. C. Strain, O. Farkas, D. K. Malick, A. D. Rabuck, K. Raghavachari, J. B. Foresman, J. V. Ortiz, Q. Cui, A. G. Baboul, S. Clifford, J. Cioslowski, B. B. Stefanov, G. Liu, A. Liashenko, P. Piskorz, I. Komaromi, R. L. Martin, D. J. Fox, T. Keith, M. A. Al-Laham, C. Y. Peng, A. Nanayakkara, M. Challacombe, P. M. W. Gill, B. Johnson, W. Chen, M. W. Wong, C. Gonzalez, J. A. Pople, *Gaussian 03, Revision E.01*, Gaussian Inc., Wallingford, CT **2004**.

[83] C. Møller, M. S. Plesset, *Phys. Rev.* **1934**, *46*, 618.

[84] J. A. Pople, J. S. Binkley, R. Seeger, *Int. J. Quantum Chem.* **1976**, *10*, 1.

[85] A. D. McLachlan, M. A. Ball, *Rev. Mod. Phys.* **1964**, *36*, 844.

[86] D. J. Rowe, *Rev. Mod. Phys.* **1968**, *40*, 153.

[87] J. Oddershede, P. Jørgensen, D. L. Yeager, *Comput. Phys. Rep.* **1984**, *2*, 33.

[88] S. P. A. Sauer, *J. Phys. B* **1997**, *30*, 3773.

[89] H. Kjær, S. P. A. Sauer, J. Yury, Y. Rusakov, L. B. Krivdin, *Chem. Phys.* **2011**, *381*, 35.

[90] T. W. Keal, D. P. Tew, D. J. Tozer, *J. Chem. Phys.* **2004**, *121*, 5654.

[91] T. H. Dunning, Jr, *J. Chem. Phys.* **1989**, *90*, 1007.

[92] D. E. Woon, T. H. Dunning, Jr, *J. Chem. Phys.* **1993**, *98*, 1358.

[93] R. A. Kendall, T. H. Dunning, Jr, R. J. Harrison, *J. Chem. Phys.* **1992**, *96*, 6796.

[94] F. Jensen, *J. Chem. Theory Comput.* **2006**, *2*, 1360.

[95] F. Jensen, *Theo. Chem. Acc.* **2010**, *126*, 371.

[96] P. F. Provasi, G. A. Aucar, S. P. A. Sauer, *J. Chem. Phys.* **2001**, *115*, 1324.

[97] V. Barone, P. F. Provasi, J. E. Peralta, J. P. Snyder, S. P.A. Sauer, R. H. Contreras, *J. Phys. Chem. A* **2003**, *107*, 4748.

[98] J. E. Peralta, G. E. Scuseria, J. R. Cheeseman, M. Frisch, *J. Chem. Phys. Lett.* **2003**, *375*, 452.

[99] K. Aidas, C. Angeli, K. L. Bak, V. Bakken, R. Bast, L. Boman, O. Christiansen, R. Cimiraglia, S. Coriani, P. Dahle, E. K. Dalskov, U. Ekström, T. Enevoldsen, J. J. Eriksen, P. Ettenhuber, B. Fernández, L. Ferrighi, H. Fliegl, L. Frediani, K. Hald, A. Halkier, C. Hättig, H. Heiberg, T. Helgaker, A. C. Hennum, H. Hettema, E. Hjertenæs, S. Høst, I.-M. Høyvik, M. F. Iozzi, B. Jansik, H. J. Aa. Jensen, D. Jonsson, P. Jørgensen, J. Kauczor, S. Kirpekar, T. Kjærgaard, W. Klopper, S. Knecht, R. Kobayashi, H. Koch, J. Kongsted, A. Krapp, K. Kristensen, A. Ligabue, O. B. Lutnæs, J. I. Melo, K. V. Mikkelsen, R. H. Myhre, C. Neiss, C. B. Nielsen, P. Norman, J. Olsen, J. M. H. Olsen, A. Osted, M. J. Packer, F. Pawlowski, T. B. Pedersen, P. F. Provasi, S. Reine, Z. Rinkevicius, T. A. Ruden, K. Ruud, V. Rybkin, P. Salek, C. C. M. Samson, A. Sánchez de Merás, T. Saue, S. P. A. Sauer, B. Schimmelpfennig, K. Sneskov, A. H. Steindal, K. O. Sylvester-Hvid, P. R. Taylor, A. M. Teale, E. I. Tellgren, D. P. Tew, A. J. Thorvaldsen, L. Thøgersen, O. Vahtras, M. A. Watson, D. J. D. Wilson, M. Ziolkowski, H. Ågren, WIREs Comput. Mol. Sci. **2014**, *4*, 269.

[100] M. J. Frisch, G. W. Trucks, H. B. Schlegel, G. E. Scuseria, M. A. Robb, J. R. Cheeseman, J. A. Montgomery, Jr, T. Vreven, K. N. Kudin, J. C. Burant, J. M. Millam, S. S. Iyengar, J. Tomasi, V. Barone, B. Mennucci, M. Cossi, G. Scalmani, N. Rega, G. A. Petersson, H. Nakatsuji, M. Hada, M. Ehara, K. Toyota, R. Fukuda, J. Hasegawa, M. Ishida, T. Nakajima, Y. Honda, O. Kitao, H. Nakai, M. Klene, X. Li, J. E. Knox, H. P. Hratchian, J. B. Cross, V. Bakken, C. Adamo, J. Jaramillo, R. Gomperts, R. E. Stratmann, O. Yazyev, A. J. Austin, R. Cammi, C. Pomelli, J. W. Ochterski, P. Y. Ayala, K. Morokuma, G. A. Voth, P. Salvador, J. J. Dannenberg, V. G. Zakrzewski, S. Dapprich, A. D. Daniels, M. C. Strain, O. Farkas, D. K. Malick, A. D. Rabuck, K. Raghavachari, J. B. Foresman, J. V. Ortiz, Q. Cui, A. G. Baboul, S. Clifford, J. Cioslowski, B. B. Stefanov, G. Liu, A. Liashenko, P. Piskorz, I. Komaromi, R. L. Martin, D. J. Fox, T. Keith, M. A. Al-Laham, C. Y. Peng, A. Nanayakkara, M. Challacombe, P. M. W. Gill, B. Johnson, W. Chen, M. W. Wong, C. Gonzalez, J. A. Pople, *Gaussian 09*, *Revision A*, *02*, Gaussian Inc., Wallingford, CT **2009**.

[101] D. Feller, *J. Comput. Chem.* **1996**, *17*, 1571.

[102] K. L. Schuchardt, B. T. Didier, T. Elsethagen, L. Sun, V. Gurumoorthi, J. Chase, J. Li, T. L. Windus, *J. Chem. Inf. Model.* **2007**, *47*, 1045.

[103] N. F. Ramsey, *Phys. Rev.* **1953**, *91*, 303.

[104] C. T. Falzon, F. Wang, *J. Chem. Phys.* **2005**, *123*, 214307.

[105] P. D. Godfrey, R. D. Brown, *J. Am. Chem. Soc.* **1995**, *117*, 2019.

[106] A. G. Csaśzaŕ, *J. Am. Chem. Soc.* **1992**, *114*, 9568.

[107] S. J. McGlone, P. S. Elmes, R. D. Brown, P. D. Godfrey, *J. Mol. Struct.* **1999**, *225–238*, 485.

[108] S. G. Stepanian, I. D. Reva, E. D. Radchenko, M. T. S. Rosado, M. L. T. S. Duarte, R. Fausto, L. Adamowicz, *J. Phys. Chem. A* **1998**, *102*, 1041.

[109] K. Iijima, K. Tanaka, S. Onuma, *J. Mol. Struct.* **1991**, *246*, 257.

[110] C. Hu, M. Shen, H. F. Schaefer, III, *J. Am. Chem. Soc.* **1993**, *115*, 2923.

[111] J. E. Del Bene, J. Elguero, *Magn. Reson. Chem.* **2004**, *42*, 421.

[112] J. E. Del Bene, J. Elguero, *J. Phys. Chem. A* **2004**, *108*, 11762.

[113] L. Rincón, R. Almeida, D. García-Aldea, *Int. J. Quantum Chem.* **2005**, *102*, 443.

[114] S. A. Kulkarni, L. J. Bartolotti, R. K. Pathak, *Chem. Phys. Lett.* **2003**, *372*, 620.

How to cite this article: Chaudhuri P, Canuto S, Provasi PF. NMR spin–spin coupling constants in hydrogen-bonded glycine clusters. *Int J Quantum Chem*. 2018;e25608. https://doi.org/10.1002/qua.25608